Soft Matter

Worm-Globule Transition of Amphiphilic pH-Responsive Heterografted Bottlebrushes at Air-Water Interface

Journal:	*Soft Matter*
Manuscript ID	SM-ART-12-2023-001635.R1
Article Type:	Paper
Date Submitted by the Author:	08-Jan-2024
Complete List of Authors:	Kelly, Michael; University of Tennessee, Chemistry Zhao, Bin; The University of Tennessee, Department of Chemistry

SCHOLARONE™
Manuscripts

Worm-Globule Transition of Amphiphilic pH-Responsive Heterografted Bottlebrushes at Air-Water Interface

*Michael T. Kelly and Bin Zhao**

Department of Chemistry, University of Tennessee, Knoxville, TN 37996, United States

* Corresponding author. Email: bzhao@utk.edu (B.Z.)

Abstract: Heterografted molecular bottlebrushes (MBBs) with side chains composed of poly(*n*-butyl acrylate) (P*n*BA) and pH-responsive poly(2-(*N*,*N*-diethylamino)ethyl methacrylate) (PDEAEMA, pK_a = 7.4) have been shown to be efficient, robust, and responsive emulsifiers. However, it remains unknown how they respond to external stimuli at interfaces. In this work, the shape-changing behavior of six hetero- and homografted MBBs at air-water interfaces in response to pH changes and lateral compression was investigated using a Langmuir-Blodgett trough and atomic force microscopy. At a surface pressure of 0.5 mN/m, PDEAEMA-containing MBBs showed no worm-globule transitions when the pH was increased from 4.0 to 10.0, at which PDEAEMA becomes insoluble in water. Upon lateral compression at pH 4.0, MBBs with a mole fraction of PDEAEMA side chains ($x_{PDEAEMA}$) < 0.50 underwent pronounced worm-globule shape transitions; there was an increasing tendency for bottlebrushes to become connected with increasing $x_{PDEAEMA}$. At $x_{PDEAEMA}$ = 0.76, the molecules remained wormlike even at high compression. These observations were presumably caused by the increased electrostatic repulsion between protonated PDEAEMA side chains in the subphase with increasing $x_{PDEAEMA}$, hindering the shape change. At pH 10.0, MBBs with $x_{PDEAEMA}$ < 0.50 showed a lower tendency to change

their wormlike morphologies upon compression than at pH 4.0. No shape transition was observed when $x_{PDEAEMA} > 0.50$, attributed to the relatively high affinity toward water and the rigidity of PDEAEMA. This study revealed the shape-changing behavior of amphiphilic pH-responsive MBBs at air-water interfaces, which could be useful for future design of multicomponent MBBs for potential applications.

Introduction

Molecular bottlebrushes (MBBs) are architecturally complex copolymers comprising relatively short polymeric side chains densely end-tethered on a backbone polymer.[1-5] The brush structure imposes strong steric interactions among the side chains, forcing the backbone of MBBs to assume an extended conformation. When the aspect ratio, that is, N_{BB}/N_{SC}, where N_{BB} is the degree of polymerization (DP) of the backbone and N_{SC} is the DP of side chains, is sufficiently high, MBBs exhibit cylindrical conformations,[1-6] resembling bottlebrush flowers and brushes for bottles and pipes. Brush polymers have attracted considerable interest in recent years, from synthesis to study of structures and assemblies;[7-22] many unique characteristics have been revealed, such as large and tunable persistence length, no backbone entanglements, and unusual crystal habits.[1-25] A variety of potential applications of MBBs have been demonstrated, ranging from photonic crystals to drug delivery systems, lubricants, and emulsion stabilizers.[26-37]

One intriguing characteristic of cylindrical MBBs is that they can undergo stimuli-induced large and abrupt conformational changes from wormlike to globular and vice versa in solution and at interfaces.[2-4,38-53] Shape-changing bottlebrush polymers are not only scientifically interesting but also have potential in applications such as medicine and stimuli-responsive emulsions.[28,37,45] Using a Langmuir-Blodgett (LB) trough, Sheiko et al. were the first to report reversible rod-globule transitions of MBBs with densely grafted poly(*n*-butyl acrylate) (P*n*BA) side chains on the water surface.[38] P*n*BA side chains spread readily on the water interface, presumably with the ester groups being in direct contact with water and the butyl tails pointing to air. Upon lateral compression, a portion of P*n*BA side chains desorbed from the air-water interface, causing the rodlike brushes to transform into globules on the water surface.[38] Subsequently, rod/star-globule shape transitions of P*n*BA MBBs were also realized at air-liquid interfaces by changing the

subphase's surface tension and on solid substrates by exposing the brushes to different vapors.[39-42] On the other hand, Schmidt et al. demonstrated temperature-induced wormlike-globular transitions by MBBs with thermoresponsive poly(*N*-isopropylacrylamide) (PNIPAm) side chains.[43] However, the collapsed globular PNIPAm brushes were unstable and eventually aggregated and precipitated out from water. This issue is particularly severe for the pH-responsive poly(2-(*N*,*N*-diethylamino)ethyl methacrylate) (PDEAEMA) brush polymer,[49] which precipitated out immediately even at rather low concentrations when the pH of the solution was increased from below to above its pK_a of ~ 7.4.[54,55] By introducing a second, soluble polymer into the side chains, either as a 2nd set of side chains in heterografted MBBs or as the outer block of diblock copolymer side chains in homografted MBBs, as a stabilizer, worm/star-stable globule shape transitions were achieved in dilute and moderately concentrated aqueous solutions.[47-53]

More recently, we showed that amphiphilic heterografted P*n*BA/PDEAEMA MBBs with proper side chain compositions are efficient and robust pH-responsive emulsifiers.[37] At pH = 4.0, PDEAEMA was protonated and soluble in water. The brushes adsorbed to the water-toluene interface and re-configured into a Janus architecture, with charged PDEAEMA side chains extending into the aqueous phase and P*n*BA residing in toluene, resulting in stable emulsions even at a polymer concentration of 0.005 wt%. When the pH was increased to 10.0, above the pK_a, PDEAEMA became insoluble in water but soluble in toluene; the brushes desorbed from the interface to the toluene phase and the emulsions were broken. The emulsion formation and disruption can be repeated at least 10 times, and the MBBs remained intact. Intriguingly, we observed that the water-toluene interface stabilized by MBBs at pH = 4.0 wrinkled when the interfacial area was reduced by withdrawing of pendant toluene droplets in acidic water or by solvent evaporation. This indicated that the brush molecules were irreversibly adsorbed at the

interface, exhibiting solidlike characteristics. When the interfacial area was decreased, the brushes experienced an in-plane lateral compression. Did they change their shape from wormlike to globular to accommodate smaller interfacial areas as homografted P*n*BA MBBs do on the water surface? In the emulsion study, the pH was cycled between acidic and basic. When the pH was increased from 4.0 to 10.0, did the brushes adsorbed at the interface collapse into a globular conformation before desorption or simply detach from the interface in a wormlike conformation?

Understanding the interfacial behavior of multicomponent MBBs will facilitate their potential uses in applications such as emulsions,[34-37,56] bijels,[57] foams,[58] etc. Motivated by the above questions, we investigated the behavior of four heterografted P*n*BA/PDEAEMA and two homografted MBBs at the air-water interface in an LB trough in response to pH changes and lateral compression (Scheme 1). We found that the shape-changing behavior of heterografted MBBs at the interface was mainly determined by the side chain composition. Although this study does not directly correlate with the behavior of amphiphilic pH-responsive heterografted MBBs at the water-toluene interface, the results have improved our understanding of multicomponent MBBs and will be useful for future design of bottlebrush polymers as interface stabilizers for various potential applications.[56-58]

Scheme 1. Shape-Changing Behavior of Heterografted P*n*BA/PDEAEMA MBBs at Air-Water Interfaces in Response to pH Changes and Lateral Compression

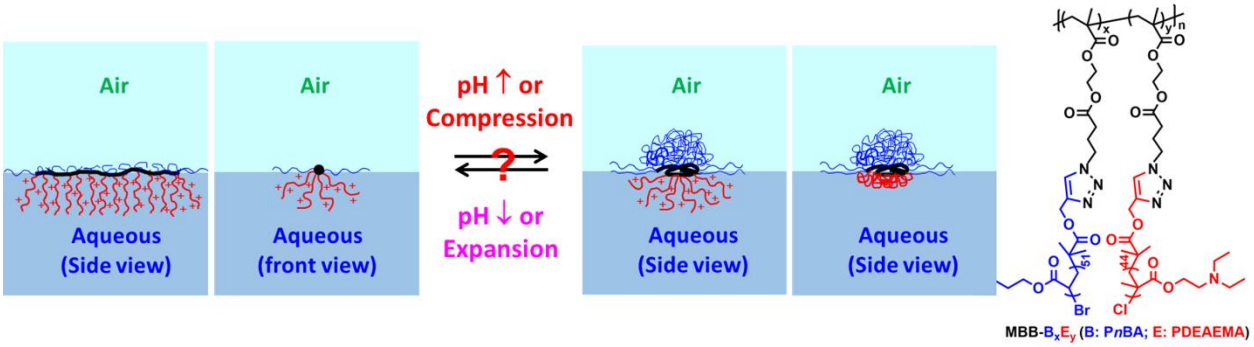

Experimental Section

Materials

Toluene (certified ACS) and monobasic potassium phosphate (99+%, Acros) were purchased from Fisher Scientific. Absolute ethanol (100%) was purchased from Decon Labs. Water was purified by a Millipore filtration device (Milli-Q). The 1.0 mM aqueous phosphate buffer solution was prepared using appropriate amounts of monopotassium phosphate and Milli-Q water. The brush polymers used in this work were prepared by grafting alkyne-end-functionalized side chain polymers onto an azide-functionalized backbone polymer using the copper(I)-catalyzed alkyne-azide cycloaddition click reaction (CuAAC).[37,45,53] The details about the synthesis and characterization can be found in a previous publication.[37] For convenience, the characterization data for the six brush polymers are included in the Supporting Information (Table S1).

Langmuir-Blodgett Lateral Compression and Sample Transfer

The compression/decompression isotherm and dipping experiments were performed using a KSV NIMA LB trough (Biolin Scientific). Prior to each experiment, the LB trough and barriers were cleaned by gently brushing the surfaces with ethanol and rinsing with Milli-Q water; nitrogen flow and an aspirator were used to remove any residual water. The platinum Wilhelmy plate was cleaned by first rinsing with ethanol and water sequentially and then being held in the flame of a Bunsen burner for several seconds until the plate was red-hot. The LB trough was assembled, and the subphase was gently poured in. The pH of the 1.0 mM phosphate subphase was adjusted prior to addition to the trough and monitored by a pH meter (Accument AB-15, calibrated using a series of buffer standards with pH values of 4.01, 7.00, and 10.01). To ensure that the water surface was sufficiently clean, the barriers were compressed several times and an aspirator was used to remove any possible surface contaminants. The surface was considered sufficiently clean if the surface

pressure (π) increase was < 0.3 mN/m during the compression process. For dipping experiments, the MBBs were transferred onto 12 mm cover glasses (Fisherbrand), which were cleaned in a "Piranha" solution (98% H_2SO_4 and 30% H_2O_2, 70/30, v/v. Caution: it reacts violently with organics and must be handled with great care!), rinsed thoroughly with Milli-Q water, and stored in isopropanol. Prior to deposition, the cover glasses were dried with a gentle nitrogen stream.

MBB solutions were prepared by dissolving the MBBs in $CHCl_3$ at a concentration of 0.5 mg/mL. In a typical experiment, 40 µL of an MBB solution was deposited gently on the water surface dropwise using a microsyringe. To ensure the complete evaporation of $CHCl_3$ and uniform spreading of the brush molecules, the system was equilibrated for at least 15 min. The barriers were then compressed at a rate of 10 mm/min. For isotherm experiments, the barriers were compressed to a desired mean molecular area and then expanded, followed by an additional cycle. For dipping experiments, the barriers were compressed to a desired surface pressure (π). Once π was steady, the glass coverslip was lifted out of the subphase at a rate of 5 mm/min while π was held constant. The coverslip was transferred to a stainless-steel disc with double sided tape to prepare for atomic force microscopy imaging.

Atomic Force Microscopy (AFM)

MBBs were imaged by AFM using a Digital Instruments Multimode IIIa Scanning Probe Microscope in tapping mode at ambient conditions. Silicon AFM probes with a reflective aluminum coating (Tap300Al-G, Budget Sensors) were used with a tip radius of 10 nm, force constant of 40 N/m, and resonance frequency of 300 kHz. The collected images were flattened, and the height scale was adjusted using Nanoscope Analysis 2.0 (Bruker). The lengths of MBBs were measured using ImageJ.

Results and Discussion

pH Effect on Morphologies of Heterografted P*n*BA/PDEAEMA MBBs on the Water Surface

Four heterografted P*n*BA/PDEAEMA and two homografted linear brush polymers (Scheme 1), MBB-$B_{1.00}E_{0.00}$, MBB-$B_{0.80}E_{0.20}$, MBB-$B_{0.64}E_{0.36}$, MBB-$B_{0.51}E_{0.49}$, MBB-$B_{0.24}E_{0.76}$, and MBB-$B_{0.00}E_{1.00}$, were used in this study, where B and E represent P*n*BA and PDEAEMA, respectively, and the subscripts are the mole fractions of the two side chain polymers ($x_{\mathrm{P}n\mathrm{BA}}$ and x_{PDEAEMA}). These MBBs were prepared by grafting alkyne end-functionalized P*n*BA with a DP of 51 and/or PDEAEMA with a DP of 44 onto an azide-functionalized backbone polymer with a DP of 406 using the CuAAC click reaction.[37] The grafting densities of all six MBBs were high, in the range of 86.7% – 94.5% (Table S1). The unreacted side chain polymers were completely removed by fractionation, confirmed by size exclusion chromatography analysis, and the side chain composition of each heterografted MBB from ^{1}H NMR analysis was similar to the initial feed ratio.

We previously observed wormlike molecules for four heterografted brush polymers on the surface of water with a pH of 4.0,[37] and image analysis showed that the average length of brush molecules was 100.6 ± 28.2 nm for MBB-$B_{0.80}E_{0.20}$ (250 molecules), 102.4 ± 26.4 nm for MBB-$B_{0.64}E_{0.36}$ (217 molecules), 99.8 ± 26.9 nm for MBB-$B_{0.51}E_{0.49}$ (287 molecules), and 99.2 ± 30.2 nm for MBB-$B_{0.24}E_{0.76}$ (234 molecules). Despite different numbers of protonated PDEAEMA side chains per brush extending into the acidic subphase, almost identical molecular lengths were observed for these brush polymers, which can be attributed to the use of the same backbone and side chain polymers in the synthesis and the high and similar grafting densities. When the pH is increased from acidic to basic, PDEAEMA becomes insoluble in water. To probe if increasing the pH from 4.0 to 10.0 would induce wormlike-globular shape transitions of four heterografted MBBs at the air-water interface, we deposited 40 μL of a 0.5 mg/mL polymer solution in chloroform

using a microsyringe onto the surface of a 1.0 mM aqueous phosphate buffer with a pH of 10.0. After the evaporation of chloroform, the monolayer of brush molecules was compressed slightly to π = 0.5 mN/m as at pH 4.0 and transferred to a "Piranha" solution-cleaned round glass disk for imaging by AFM. Wormlike brushes were seen for all four heterografted brush polymers at pH 10.0 (Figure 1), indicating that no worm-globule transition occurred despite of the insolubility of PDEAEMA side chains in the basic subphase with a pH far above the pK_a of PDEAEMA. Image analysis showed that the average contour length of brushes was 104.6 ± 26.5 nm for MBB-$B_{0.80}E_{0.20}$ (183 molecules), 100.4 ± 20.4 nm for MBB-$B_{0.64}E_{0.36}$ (194 molecules), 102.9 ± 21.8 nm for MBB-$B_{0.51}E_{0.49}$ (167 molecules), and 97.8 ± 19.9 nm for MBB-$B_{0.24}E_{0.76}$ (205 molecules). The typical heights of these brush molecules at both pH values were similar, ~ 1.5 nm. There was no significant difference in the average lengths of each brush polymer at acidic and basic pH values, and the slight difference in length could likely be caused by the limited number of bottlebrush molecules used in the image analysis.

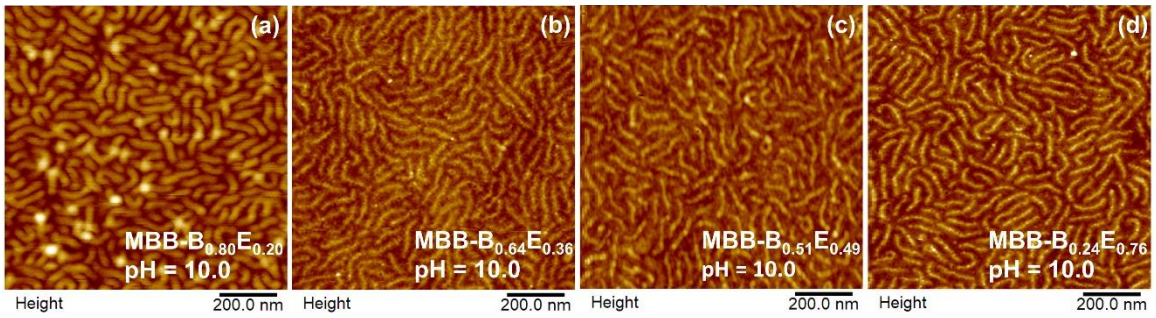

Figure 1. AFM height images of MBB-$B_{0.80}E_{0.20}$ (a), MBB-$B_{0.64}E_{0.36}$ (b), MBB-$B_{0.51}E_{0.49}$ (c), MBB-$B_{0.24}E_{0.76}$ (d) transferred onto "Piranha" solution-cleaned glass disks from the interface between air and a 1.0 mM aqueous phosphate buffer solution with a pH of 10.0 at π = 0.5 mN/m using an LB trough.

The observations for four heterografted P*n*BA/PDEAEMA MBBs were consistent with the wormlike morphology of MBB-$B_{0.00}E_{1.00}$ on the surface of a pH 10.0 aqueous solution,[37] evidencing that favorable interactions exist between PDEAEMA-containing brush molecules and

water despite the fact that PDEAEMA is insoluble in the basic solution. As mentioned earlier, we previously observed that PDEAEMA homografted bottlebrushes aggregated and precipitated out immediately from the aqueous solution upon increasing the pH from acidic to basic.[49] When a soluble polymer was introduced into the side chains as a stabilizer, the collapsed brushes took on a globular conformation.[49,51] These observations indicate that the pH-induced soluble-to-insoluble transition of PDEAEMA side chains is a very strong driving force for minimizing the contact area of the bottlebrushes with water. However, no wormlike-globular shape transition was seen for the heterografted MBBs on the water surface when the pH of the aqueous subphase was changed from 4.0 to 10.0, and MBB-$B_{0.00}E_{1.00}$ exhibited a wormlike morphology on the surface of a basic aqueous solution. Clearly, a globular shape is not the lowest energy state for PDEAEMA-containing MBBs on the surface of the basic solution. Instead, spreading of PDEAEMA side chains is favored; that is, the spreading coefficient of insoluble PDEAEMA on the surface of the pH 10.0 aqueous solution $S = \gamma_{water\text{-}air} - (\gamma_{water\text{-}PDEAEMA} + \gamma_{PDEAEMA\text{-}air}) > 0$, where $\gamma_{water\text{-}air}$ is the surface tension of the basic subphase, $\gamma_{water\text{-}PDEAEMA}$ is the interfacial free energy between the basic aqueous solution and PDEAEMA, and $\gamma_{PDEAEMA\text{-}air}$ is the surface free energy of PDEAEMA. This can be attributed to the dipole-dipole and hydrogen bonding interactions of water with the ester and tertiary amine groups of PDEAEMA resulting in an affinity of PDEAEMA toward water.

Shape-Changing Behavior of Heterografted P*n*BA/PDEAEMA MBBs on the Surface of a 1.0 mM Aqueous Phosphate Buffer with a pH of 4.0 in Response to Lateral Compression

Before investigating how heterografted P*n*BA/PDEAEMA MBBs at the air-water interface responded to lateral compression and expansion at the subphase pH values of 4.0 and 10, we examined the behavior of MBB-$B_{1.00}E_{0.00}$ on the water surface in an LB trough. Sheiko et al. previously reported that P*n*BA bottlebrushes with sufficiently long P*n*BA side chains underwent

reversible rod-globule shape transitions upon lateral compression.[38] Figure S1a shows the surface pressure (π)-mean area per brush molecule (A) isotherms for two cycles of lateral compression and decompression, which are identical. Upon compression, π began to increase at $A_0 = 2.57 \times 10^3$ nm^2/brush, which is the mean area occupied by one brush molecule prior to conformational changes obtained by linear extrapolation, and increased rapidly and almost linearly with decreasing A until A reached ~ 2000 nm^2/brush. A plateau was observed subsequently, followed by a rise in π and then a second plateau at A = ~ 1300 nm^2/brush. AFM samples were prepared by transferring the brush monolayer onto glass disks at different π values. At π = 0.50 mN/m, the P*n*BA brushes were wormlike with an average length of 100.1 ± 23.6 nm (Figure S1b). When π was increased to 18 mN/m (Figure S1c), the molecules shrank significantly. At π = 19 mN/m (Figure S1d), which was located in the middle of the first plateau, the vast majority of bottlebrushes transformed into globules, although not very round. Some molecules exhibited tadpole-like conformations, suggesting that the worm-to-globule transition was likely initiated from the brush's ends. When π reached 20 mN/m, near the end of the first plateau, all the brushes completed the shape transition (Figure S1e), and the globules were stabilized against aggregation by the side chains that remained adsorbed on the water surface.[38] Upon decompression to π = 0.50 mN/m, the brushes resumed wormlike but appeared to be wavier than the initial morphology (Figure S1f), which may be an artifact of the unfolding process. The overall behavior of this brush polymer is similar to that reported by Sheiko et al.[38] Note that the conformations of the bottlebrushes might change during the transfer process from the air-water interface to glass disks. However, we believe that the morphologies of MBBs observed by AFM correspond to those on the water surface based on the following. (i) The brush molecules exhibit distinct morphologies at different degrees of lateral compression (i.e., different π values), which correlated well with the π-A isotherm data. Upon

expansion to π = 0.50 mN/m, the brushes returned to the wormlike morphology, though wavier. (ii) Our results for MBB-$B_{1.00}E_{0.00}$ are consistent with those reported by Sheiko et al.[38] (iii) We previously reported that drop casting of 3-arm star brushes at different conditions gave morphologies, either starlike or globular, consistent with the dynamic light scattering and ^{1}H NMR analysis results.[52] In addition, we used photocrosslinking to fix the morphology of globular bottlebrushes in solution and found from AFM imaging that the molecules were globular under the conditions where non-crosslinked MBBs exhibited wormlike conformations.[50] Considering all of these, we believe that the morphologies of MBBs were preserved during the transfer to the solid substrates for imaging under the carefully chosen conditions with right tools and procedures. We also note here that other types of bottlebrushes and star copolymers have been reported to exhibit rich and complex conformational behaviors at the interfaces.[59-62]

We then studied the behavior of heterografted P*n*BA/PDEAEMA MBBs on the surface of a 1.0 mM phosphate buffer with a pH of 4.0. Figure 2 shows the LB isotherms for two cycles of compression and expansion and AFM images at different surface pressures for MBB-$B_{0.80}E_{0.20}$. Two plateaus can be discerned from both π-A isotherms for this brush polymer upon lateral compression. In the first cycle, π started to increase at A_0 = 2500 nm^2/brush. After decompression, in contrast to MBB-$B_{1.00}E_{0.00}$, a large hysteresis was observed, where π did not return to ~ 0 mN/m but ended at ~ 3 mN/m (Figure 2a). This hysteresis was presumably caused by the loose attachment of brushes with charged PDEAEMA side chains on the platinum Wilhelmy plate likely through charge-induced charge interactions at the metal surface.[63] AFM showed that the bottlebrushes were worm- or rod-like at π = 0.50 mN/m (Figure 2b). Note that for this sample on the surface of the acidic solution, 20% of the side chains are charged PDEAEMA, which extended into the subphase. Once transferred onto the glass disk, the charged side chains interacted strongly with the substrate,

and the brushes were likely pinned on the glass disk immediately. At π = 19 mN/m (Figure 2c), which was at the beginning of the first plateau, some brushes already changed into a globular shape, while other molecules remained wormlike. Upon further increasing π to 22 mN/m, nearly all brushes transformed into globules (Figure 2d). Upon decompression, the globular molecules were unfolded into a wormlike morphology (Figure 2e). This heterografted brush polymer behaved similarly to MBB-$B_{1.00}E_{0.00}$, with the only noticeable difference being the hysteresis observed in the first compression/decompression cycle.

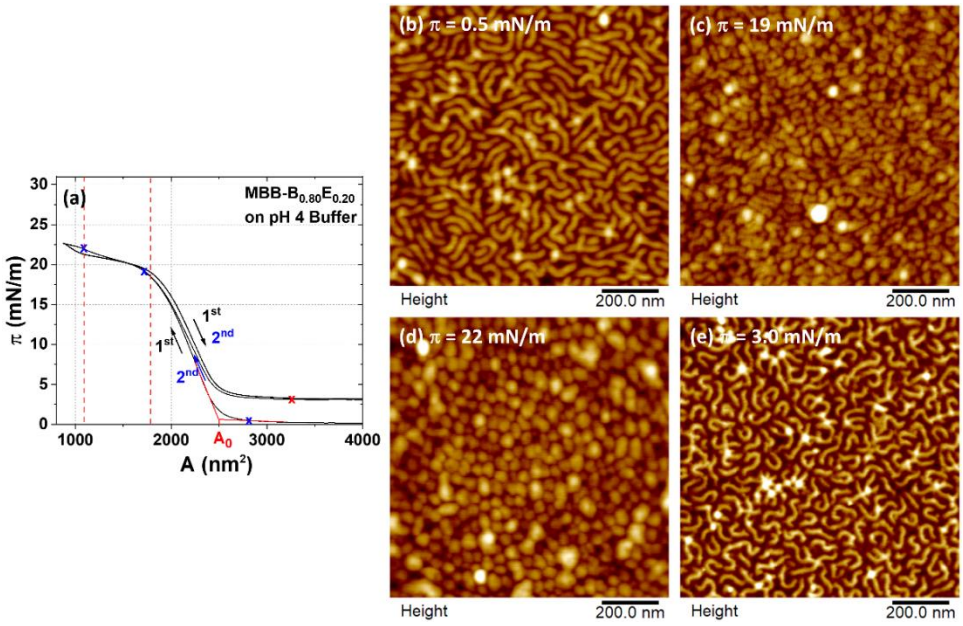

Figure 2. (a) Surface pressure (π)-mean area per brush (A) isotherms from two cycles of compression and expansion for MBB-$B_{0.80}E_{0.20}$ on the surface of a 1.0 mM aqueous phosphate buffer with a pH of 4.0 and AFM images of MBB-$B_{0.80}E_{0.20}$ at different surface pressures: (b) π = 0.5 mN/m, (c) π = 19 mN/m, (d) π = 22 mN/m, and (e) π = 3.0 mN/m.

Figure 3a shows the π-A isotherms from two cycles of compression and expansion for MBB-$B_{0.64}E_{0.36}$, with A_0 being at 2470 nm^2/brush from the first cycle for this brush polymer. While the first plateau was visible, we only saw the beginning of the transition from the 1st plateau to a possible second one. The brushes were wormlike at π = 0.5 mN/m (Figure 3b) and 20 mN/m (Figure 3c); the molecular worms were more closely packed at π = 20 mN/m. At π = 23 mN/m,

the molecules transformed to globular (Figure 3d); however, the globules were less defined and less round than those in Figures 2d and some brushes were partially collapsed, despite the surface pressure being at the end of the plateau. Upon expansion, the brushes returned to be wormlike (Figure 3e).

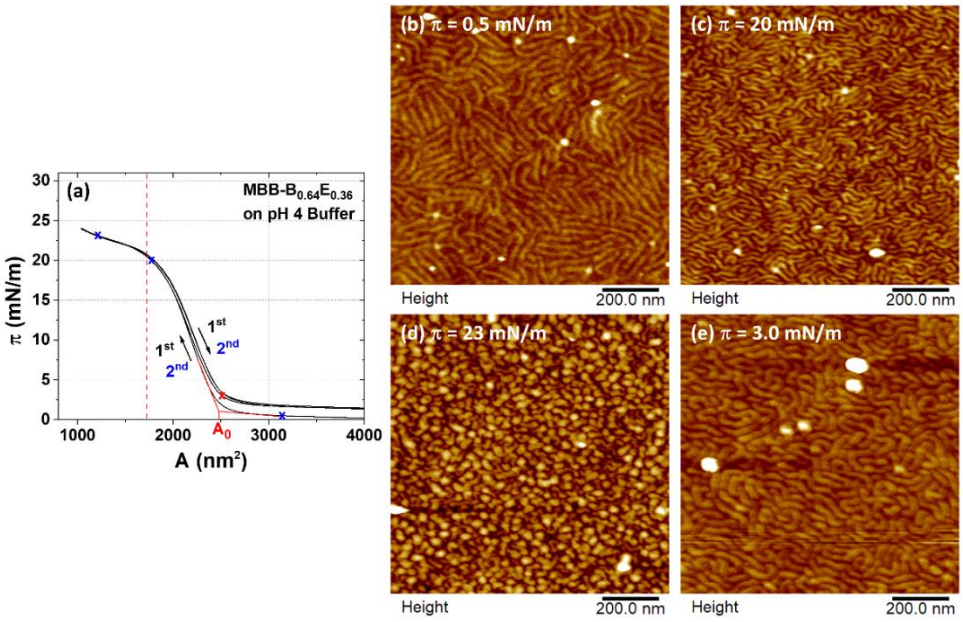

Figure 3. (a) Surface pressure (π)-mean area per brush (A) isotherms from two cycles of compression and expansion for MBB-$B_{0.64}E_{0.36}$ on the surface of a 1.0 mM aqueous phosphate buffer with a pH of 4.0 and AFM images of MBB-$B_{0.64}E_{0.36}$ at different surface pressures: (b) π = 0.5 mN/m, (c) π = 20 mN/m, (d) π = 23 mN/m, and (e) π = 3.0 mN/m.

Further increasing $x_{PDEAEMA}$ in the side chains of MBBs to 0.49, the LB isotherms of the heterografted brushes (MBB-$B_{0.51}E_{0.49}$) at pH 4.0 showed an even weaker transition from the rapid rise region to the plateau, as evidenced by the more upward-pointing curve from A = ~ 1700 to ~ 1100 nm^2/brush (Figure 4a). There seems no sign that the second plateau will appear if the compression continues. However, A_0 was 2500 nm^2/brush, which showed little change from the first two heterografted brush polymers. AFM revealed that MBB-$B_{0.51}E_{0.49}$ was wormlike at π = 0.5 mN/m (Figure 4b) as other MBBs and was about to collapse at π = 21 mN/m (Figure 4c). At π = 24 mN/m, the brush molecules were globular but more connected (Figure 4d); individual

molecules were harder to be discerned than MBB-$B_{0.64}E_{0.36}$ in Figure 3d. Despite the observation that the brush molecules seemingly aggregated at π = 24 mN/m, they returned to the wormlike state upon decompression to π = 3.5 mN/m (Figure 4e).

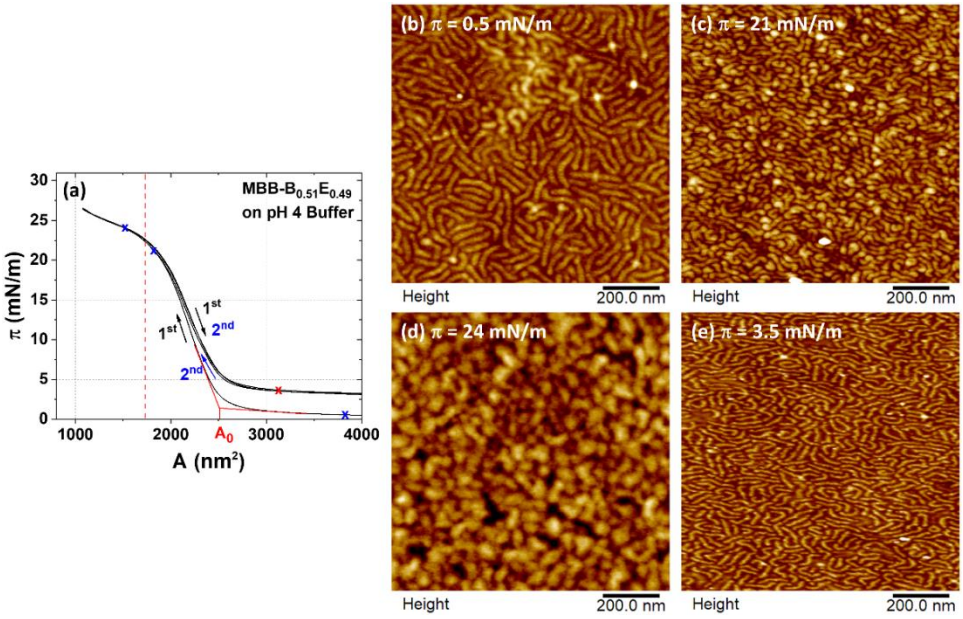

Figure 4. (a) Surface pressure (π)-mean area per brush (A) isotherms from two cycles of compression and expansion for MBB-$B_{0.51}E_{0.49}$ on the surface of a 1.0 mM aqueous phosphate buffer with a pH of 4.0 and AFM images of MBB-$B_{0.51}E_{0.49}$ bottlebrushes at different surface pressures: (b) π = 0.5 mN/m, (c) π = 21 mN/m, (d) π = 24 mN/m, and (e) π = 3.5 mN/m.

For MBB-$B_{0.24}E_{0.76}$ with $x_{PDEAEMA}$ of 76%, no transition in the π-A isotherms was observed upon compression (Figure 5a); the isotherms showed a sharp, monotonous increase in π with reducing A. Similar to other PDEAEMA-containing heterografted MBBs, there was a large hysteresis in the isotherm in the first compression-decompression cycle, but the hysteresis was negligible in the second cycle. From the AFM images, the brushes stayed in the cylindrical wormlike state from π = 0.5 to 30 mN/m (Figure 5b,c,d); they were simply more closely packed at higher surface pressures, and the film became smoother. Unexpectedly, no molecular worms could be discerned from the AFM images after decompression to π = 3.5 mN/m; the brushes seemed to "fuse" into a featureless film (Figure 5e), presumably because the sufficiently large

number of charged PDEAEMA side chains from neighboring bottlebrushes interdigitated and consequently, the brushes could not separate from each other on the time scale of expansion. We repeated the LB and AFM experiments for this polymer at pH 4.0 and confirmed this observation.

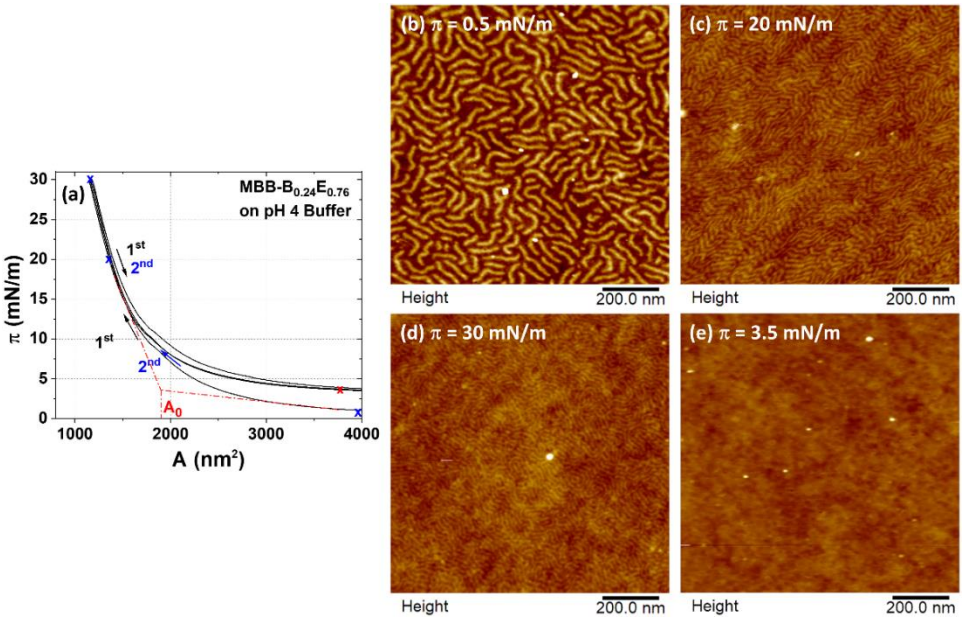

Figure 5. (a) π-A isotherms from two compression-decompression cycles for MBB-$B_{0.24}E_{0.76}$ on the surface of a 1.0 mM phosphate buffer at pH 4.0 and AFM images of MBB-$B_{0.24}E_{0.76}$ at different surface pressures: (b) π = 0.5 mN/m, (c) π = 20 mN/m, (d) π = 30 mN/m, and (e) π = 3.5 mN/m.

From Figures 2 – 5, several trends can be seen for the conformational behavior of heterografted P*n*BA/PDEAEMA MBBs on the surface of the pH 4.0 phosphate solution. (i) With increasing $x_{PDEAEMA}$ in the side chains, the transition in the π-A isotherm of MBBs from the rapid increase region to a plateau became weaker and eventually vanished. (ii) With increasing $x_{PDEAEMA}$, the tendency of MBBs to undergo a unimolecular worm-to-globule shape transition in response to lateral compression decreased, and the tendency for bottlebrushes to become connected initially increased and then decreased. (iii) At a sufficiently high $x_{PDEAEMA}$, the brush molecules showed no tendency to change their shape from wormlike to globular.

Shape-Changing Behavior of Heterografted P*n*BA/PDEAEMA MBBs on the Surface of a 1.0 mM Aqueous Phosphate Buffer with a pH of 10.0 in Response to Lateral Compression

Figure 1 shows that all four heterografted MBBs exhibited wormlike morphologies on the surface of a 1.0 mM phosphate solution with a pH of 10.0, where PDEAEMA side chains were insoluble in water and presumably spread on the water surface due to the attractive interactions of polar groups with water along with P*n*BA side chains. Thus, this situation is very different from pH 4.0, where PDEAEMA side chains are protonated and extend into the acidic subphase. We were also very interested in how wormlike heterografted P*n*BA/PDEAEMA MBBs with both side chain polymers spreading on the surface of a basic solution responded to mechanical compression and decompression. Figure 6a shows the π-A isotherms of MBB-$B_{0.80}E_{0.20}$ on the surface of a 1.0 mM phosphate solution with a pH of 10.0, which are similar to those of the same polymer at pH 4.0 (Figure 2a). Two plateaus can be seen in the higher π region, although the transition from the first one to the second is not very pronounced. The value of A_0 was 2600 nm^2/brush, slightly higher than that at pH 4.0 (2500 nm^2/brush). Similar to Figure 1a, the molecules were wormlike at π = 0.5 mN/m (Figure S2b), while at π = 19 mN/m, the bottlebrushes were about to collapse or partially collapsed (Figure S2c). When π reached 21 mN/m, the brushes transformed to globules (Figure 6b). After π decreased to ~ 0.5 mN/m, the brushes changed back to wormlike (Figure S2d).

The π-A isotherms of MBB-$B_{0.64}E_{0.36}$ at pH 10.0 shown in Figure 6c are also similar to those at pH 4.0. The value of A_0 from extrapolation was 2650 nm^2/brush, larger than that at pH 4.0 (2470 nm^2/brush). AFM showed that the bottlebrushes assumed a cylindrical morphology at π = 0.5 mN/m (Figure S3b) and began the conformational change at π = 22 mN/m (Figure S3c). Further compressing the film to π = 23 mN/m, the collapsed brushes became connected with each other (Figure 6d) and seemed to be more aggregated than the same MBB on the acidic water surface at the same surface pressure (Figure 3d). Despite the apparent aggregation, the brushes returned to the wormlike morphology after decompression (Figure S3d).

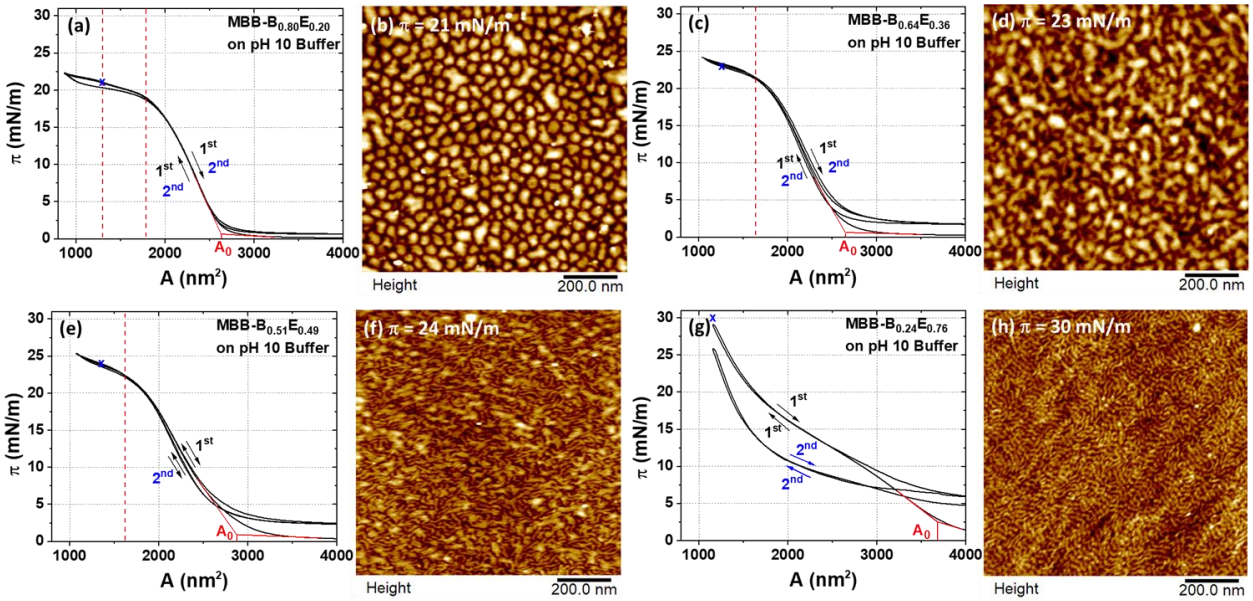

Figure 6. π-A isotherms from two compression-expansion cycles for (a) MBB-$B_{0.80}E_{0.20}$, (c) MBB-$B_{0.64}E_{0.36}$, (e) MBB-$B_{0.51}E_{0.49}$, and (g) MBB-$B_{0.80}E_{0.20}$ on the surface of a 1.0 mM phosphate buffer at pH 10.0 and AFM images of (b) MBB-$B_{0.80}E_{0.20}$ at π = 21 mN/m, (d) MBB-$B_{0.64}E_{0.36}$ at π = 23 mN/m, (f) MBB-$B_{0.51}E_{0.49}$ at π = 24 mN/m, and (h) MBB-$B_{0.24}E_{0.76}$ at π = 30 mN/m,.

For MBB-$B_{0.51}E_{0.49}$, the isotherms at pH 10.0 are also similar to those at pH 4.0, with a weak transition from the rapid rise region to the upward-pointing plateau (Figure 6e). The brushes were wormlike before compression and after expansion as well as at π = 21 mN/m (Figure S4b,c,e). When the film was compressed to π = 24 mN/m, the vast majority of brushes remained in the wormlike state (Figure 6f). Some molecules showed a sign of changing the conformation while others started to aggregate. This is different from the same brush polymer at pH 4.0, where nearly all the bottlebrushes changed to globular conformations, though less round and somewhat connected (Figure 4d). By comparing the behavior of MBB-$B_{0.51}E_{0.49}$ and MBB-$B_{0.64}E_{0.36}$ at the two pH values, it is clear that heterografted P*n*BA/PDEAEMA MBBs had a lower tendency to undergo shape transitions at pH 10.0 and the tendency decreased with increasing $x_{PDEAEMA}$.

A large hysteresis was observed for MBB-$B_{0.24}E_{0.76}$ at pH 10.0 between the two cycles of compression and expansion (Figure 6g). In the second cycle, the hysteresis between compression

and decompression curves was small. In fact, the hysteresis in the first cycle of compression and decompression increased with increasing $x_{PDEAEMA}$, while it was negligible for the second cycle for all four samples (Figure 6). This could be attributed to the following two factors. (i) Since the pK_a of protonated PDEAEMA is ~ 7.4, there is still a small amount of charges on the brushes at pH 10.0. If the Henderson–Hasselbalch equation can be applied, 0.25% amine groups would be charged at pH 10.0. These charges would induce charges on the metal surface and thus electrostatic attractive interactions. (ii) Neutral amines are known to be good ligands for transition metals. Both factors could cause some brushes to remain adsorbed on the Pt surface after decompression. For the large hysteresis between the two cycles in Figure 6g, we speculate that it is related to the interactions between MBBs and the rearrangement of brushes to achieve close packing. Similar to the isotherms at pH = 4.0 (Figure 5a), π increased sharply and monotonously upon compression at A < 2000 nm^2/brush. A_0 was hard to determine but was estimated to be 3680 nm^2/brush from the first cycle. AFM showed no shape transition upon compression (Figure S5b,c), even at a surface pressure as high as 30 mN/m (Figure 6h), where the wormlike brushes were packed extremely tightly together. Unlike at pH 4.0, where wormlike molecules could not be discerned after expansion, individual brushes can be easily seen after decompression at pH = 10.0 (Figure S5d).

Figures 6 and S2-S5 show that in general each brush polymer behaved similarly at the two pH values and appeared to exhibit a lower tendency at the higher pH to change from a wormlike to a globular morphology. For comparison, we also investigated the behavior of MBB-$B_{0.00}E_{1.00}$ on the surface of the 1.0 mM phosphate buffer with a pH of 10.0 (Figure 7). The isotherms from two compression-decompression cycles were similar to those of MBB-$B_{0.24}E_{0.76}$ at pH 10.0. The estimated A_0 value of MBB-$B_{0.00}E_{1.00}$ from the first compression was 3800 nm^2/brush, the largest in this study. AFM revealed a wormlike morphology for the brushes at all surface pressures (Figure

7b-f), including π = 34 mN/m. Clearly, MBB-$B_{0.00}E_{1.00}$ exhibited no tendency to change the wormlike morphology on the surface of the basic solution when compressed, in stark contrast to MBB-$B_{1.00}E_{0.00}$ that readily underwent a reversible worm-globule shape transition at the air-water interface upon compression. This could be attributed to the following factors. (i) As mentioned earlier, there is still a small amount of charges on the brushes at pH 10.0 (0.25% amine groups protonated based on calculations). (ii) Both -COO- and -$N(C_2H_5)_2$ groups of PDEAEMA have dipole-dipole and hydrogen bonding interactions with water, resulting in a higher affinity of PDEAEMA toward water than P*n*BA, which may hinder the desorption of PDEAEMA side chains from the water surface. (iii) The T_g of P*n*BA is around – 50 °C, meaning that P*n*BA has a high mobility at room temperature. In contrast, PDEAEMA is glassy at room temperature and therefore has a lower segmental mobility than P*n*BA. All of these factors would increase the rigidity of the polymer, hindering the worm-globule transition. Consequently, MBB-$B_{0.00}E_{1.00}$ remained wormlike on the water surface at pH 10.0 even under rather high degrees of lateral compression.

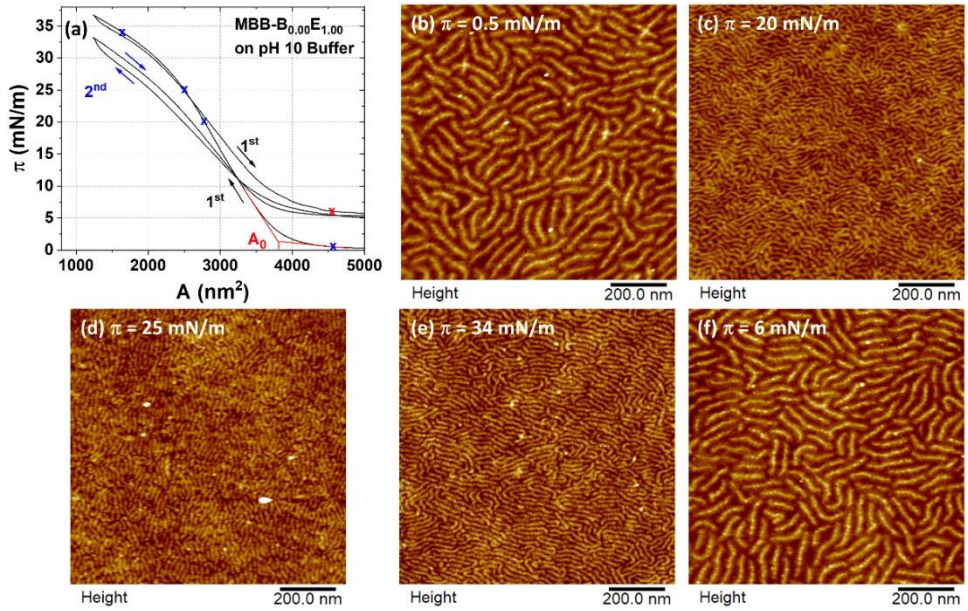

Figure 7. (a) π-A isotherms from two compression-expansion cycles for MBB-$B_{0.00}E_{1.00}$ on the surface of a 1.0 mM phosphate buffer at pH 10.0 and AFM images of MBB-$B_{0.00}E_{1.00}$ at π = 0.5 mN/m (b), 20 mN/m (c), 25 mN/m (d), 34 mN/m (e), and 6.0 mN/m after expansion (f).

Further Discussion on Shape-Changing Behavior of Heterografted P*n*BA/PDEAEMA MBBs on the Water Surface at pH 4.0 and 10.0

The estimated A_0 values for the four heterografted brush polymers at pH 4.0 and 10.0 from the first compression isotherms are plotted against $x_{PDEAEMA}$ (Figure 8), along with the data for MBB-$B_{1.00}E_{0.00}$ on Milli-Q water and MBB-$B_{0.00}E_{1.00}$ on the surface of the pH 10.0 aqueous solution. At pH 4.0, A_0 was initially almost constant when $x_{PDEAEMA}$ in the side chains was increased from 0 to 0.49 and then dropped noticeably at $x_{PDEAEMA}$ = 0.76. This may be attributed to the protonated PDEAEMA side chains extending into the aqueous subphase. When $x_{PDEAEMA}$ was < 0.50, A_0 was not significantly affected as the P*n*BA side chains were still closely packed while spreading on the water surface. At $x_{PDEAEMA}$ = 0.76, the brushes can be packed to be closer to each other at the air-water interface because few P*n*BA side chains spread on the water surface, resulting in a lower apparent A_0. In contrast, at pH = 10.0, both P*n*BA and PDEAEMA side chains were located and spread on the water surface. A_0 was found to increase with increasing $x_{PDEAEMA}$. Considering the $M_{n,cal}$ values for PDEAEMA and P*n*BA side chains (8.4 kDa and 6.7 kDa, respectively, calculated from the DPs), it is reasonable that A_0 increases with increasing $x_{PDEAEMA}$. The much larger estimated A_0 values for MBB-$B_{0.24}E_{0.76}$ and MBB-$B_{0.00}E_{1.00}$ are likely related to the large hysteresis seen in the isotherms; it is possible that the bottlebrushes were not closely packed but formed a percolated two-dimensional network at the air-water interface, making A_0 appear larger.

As can be seen from Figure S1, P*n*BA side chains can desorb from the water surface upon lateral compression, causing the worm-globule shape transition of MBB-$B_{1.00}E_{0.00}$. At pH = 4.0, PDEAEMA is protonated, and MBB-$B_{0.00}E_{1.00}$ is soluble in water, whereas at pH = 10.0, the PDEAEMA side chains of MBB-$B_{0.00}E_{1.00}$ spread on the water surface. The relatively high affinity of PDEAEMA toward water may hinder the desorption of PDEAEMA side chains from the water

surface, and the rigidity of the polymer, as discussed earlier, would make the worm-globule transition more difficult. Consequently, MBB-$B_{0.00}E_{1.00}$ remained wormlike regardless of how high the surface pressure was (Figure 7). Thus, whether heterografted P*n*BA/PDEAEMA MBBs can undergo worm-globule shape transitions at the air-water interface depends on the competition between the two side chain polymers. However, the situations at pH 4.0 and 10.0 are different and are discussed in the following.

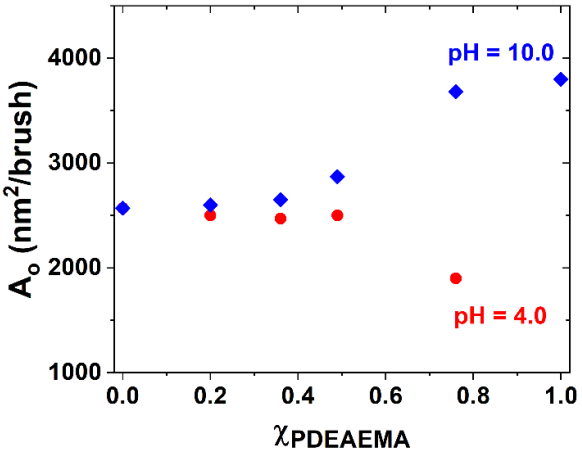

Figure 8. Plot of A_0 (nm^2/brush) vs $x_{PDEAEMA}$ in the side chains of MBBs.

When the pH is 4.0, the protonated PDEAEMA side chains extend into the subphase from the backbone and are presumably uniformly distributed in the half-cylindrical region along the backbone on the water side (Scheme 1 left) due to the electrostatic repulsive interactions and the osmotic pressure. When the brushes are compressed, the interfacial area available for each brush molecule is reduced. Some P*n*BA side chains desorb from the water surface and aggregate in air. Accordingly, the volume available to the PDEAEMA side chains in water is also reduced, and these charged side chains are forced to come closer to each other. Consequently, the electrostatic repulsive forces and the osmotic pressure increase with decreasing distance. For MBB-$B_{0.80}E_{0.20}$, MBB-$B_{0.64}E_{0.36}$, and MBB-$B_{0.51}E_{0.49}$ with $x_{PDEAEMA} < 0.50$, the electrostatic repulsive interactions among the charged side chains and the osmotic pressure appear not to be large enough to prevent

the coil-up of the backbone and the worm-globule shape transition. However, with increasing $x_{PDEAEMA}$ from 0.20 to 0.49, the transition from the rapid rise region to the plateau in the π-A isotherm occurs at higher surface pressures, i.e., greater compression is needed to overcome the electrostatic repulsive forces among the charged PDEAEMA side chains. At a lower $x_{PDEAEMA}$, the worm-globule shape transition of individual brushes is observed as in the case of MBB-$B_{0.80}E_{0.20}$. Note that the globular shape of the molecular brushes is actually a Janus globular structure with P*n*BA side chains aggregating in air and protonated PDEAEMA side chains extending into the acidic solution (Scheme 1), different from globular MBB-$B_{1.00}E_{0.00}$ molecules. For MBB-$B_{0.64}E_{0.36}$ and MBB-$B_{0.51}E_{0.49}$, due to the higher $x_{PDEAEMA}$ and the smaller number of P*n*BA side chains on the water surface, the brush molecules are squeezed to be even closer to each other; consequently, the desorbed P*n*BA side chains from neighboring brushes can merge together, and the globular brushes become increasingly connected. For MBB-$B_{0.24}E_{0.76}$, the brush molecules are compressed to be so close to each other that the charged PDEAEMA side chains from neighboring bottlebrushes likely interdigitated and the brushes are possibly fused together. As a result, the coiling of the backbone is inhibited and no worm-globule shape transition is observed.

At pH = 10.0, both P*n*BA and PDEAEMA side chains of heterografted MBBs spread on the water surface. While MBB-$B_{1.00}E_{0.00}$ exhibited a reversible worm-globule shape transition upon compression, MBB-$B_{0.00}E_{1.00}$ remained wormlike even at very high surface pressures, which are attributed to the different interaction strengths of P*n*BA and PDEAEMA side chains with water and the rigidity of PDEAEMA side chains as discussed earlier. Hence, the shape-changing behavior of P*n*BA/PDEAEMA MBBs depends on $x_{PDEAEMA}$, and the overall tendency to undergo worm-globule transitions decreases with increasing $x_{PDEAEMA}$. Individual brushes of MBB-$B_{0.80}E_{0.20}$ were observed to change their shape to globular upon compression. While MBB-

$B_{0.64}E_{0.36}$ exhibited conformational changes at both pH 4.0 and 10.0 when compressed, the globular molecules were more connected with each other at pH 10.0. MBB-$B_{0.51}E_{0.49}$ showed a significantly lower tendency to undergo a shape transition at pH 10.0 than at pH 4.0; at pH 10.0, the vast majority of the MBB-$B_{0.51}E_{0.49}$ molecules were wormlike at π = 24 mN/m, while at pH 4.0 almost all brushes turned globular at the same surface pressure, though somewhat aggregated. Like at pH 4.0, MBB-$B_{0.24}E_{0.76}$ remained in the wormlike state even at very high compression but for a different reason. Here, the relatively high affinity of PDEAEMA toward water and the rigidity of PDEAEMA make the wormlike-to-globular transition difficult.

Conclusions

Using an LB trough and AFM, we studied the shape-changing behavior of four pH-responsive heterografted P*n*BA/PDEAEMA MBBs with $x_{PDEAEMA}$ of 0.20 to 0.36, 0.49, and 0.76 on the water surface in response to pH changes and lateral compression. For comparison, MBB-$B_{1.00}E_{0.00}$ on Milli-Q water and MBB-$B_{0.00}E_{1.00}$ on the surface of a pH 10.0 solution were also investigated. No worm-globule transitions were observed for all heterografted MBBs on the water surface when the pH was increased from 4.0 to 10.0 at π = 0.5 mN/m. For MBBs on the surface of the acidic solution, worm-globule transitions were observed upon compression when the $x_{PDEAEMA}$ was < 0.50; the collapsed brushes, however, became increasingly connected with each other with increasing $x_{PDEAEMA}$. MBB-$B_{0.24}E_{0.76}$ remained wormlike even at high compression. The behavior of these MBBs at pH 4.0 is attributed to the increased repulsive interactions between protonated PDEAEMA side chains in the acidic subphase with increasing $x_{PDEAEMA}$. On the surface of the basic solution, the brushes with $x_{PDEAEMA}$ < 0.50 generally showed a lower tendency to change their shape than at pH 4.0. MBB-$B_{0.24}E_{0.76}$ and MBB-$B_{0.00}E_{1.00}$ stayed in the wormlike state even

at rather high surface pressures. These are attributed to the relatively high affinity toward water and the rigidity of PDEAEMA making the shape transition difficult. This study revealed the behavior of amphiphilic pH-responsive heterografted MBBs at the air-water interface. The understanding gained here will be beneficial to our future design of multicomponent MBBs for potential applications related to interfaces, such as emulsions, bijels, foams, and polymer blends.[56-58]

Conflicts of interest

There are no conflicts to declare.

Acknowledgements

The authors are grateful for the NSF support (NSF DMR-2004564).

Electronic supplementary information (ESI) available: characterization data for six brush polymers, π-A isotherms and additional AFM images of MBB-$B_{1.00}E_{0.00}$, MBB-$B_{0.80}E_{0.20}$, MBB-$B_{0.64}E_{0.36}$, MBB-$B_{0.51}E_{0.49}$, and MBB-$B_{0.24}E_{0.76}$ at various surface pressures.

References

1. M. Zhang and A. H. E. Müller, *J. Polym. Sci. Part A: Polym. Chem.*, 2005, **43**, 3461-3481.
2. S. S. Sheiko, B. S. Sumerlin, K. Matyjaszewski, *Prog. Polym. Sci.*, 2008, **33**, 759-785.
3. H.-i. Lee, J. Pietrasik, S. S. Sheiko, K. Matyjaszewski, *Prog. Polym. Sci.*, 2010, **35**, 24-44.
4. B. Zhao, *J. Phys. Chem. B*, 2021, **125**, 6373-6389.
5. Z. Li, M. Tang, S. Liang, M. Zhang, G. M. Biesold, Y. He, S.-M. Hao, W. Choi, Y. Liu, J. Peng, Z. Lin, *Prog. Polym. Sci.*, 2021, **116**, 101387.
6. T. Pan, S. Dutta, Y. Kamble, B. B. Patel, M. A. Wade, S. A. Rogers, Y. Diao, D. Guironnet, C. E. Sing, *Chem. Mater.*, 2022, **34**, 1990-2024.
7. H. G. Börner, K. Beers, K. Matyjaszewski, S. S. Sheiko, M. Möller, *Macromolecules*, 2001**,** **34**, 4375-4383.
8. C. Cheng, K. Qi, E. Khoshdel, K. L. Wooley, *J. Am. Chem. Soc.*, 2006, **128**, 6808–6809.
9. Y. Xia, B. D. Olsen, J. A. Kornfield, R. H. Grubbs, *J. Am. Chem. Soc.*, 2009, **131**, 18525-18532.
10. J. Rzayev, *ACS Macro Lett.*, 2012**,** **1**, 1146-1149.

11. Y. Li, J. Zou, B. P. Das, M. Tsianou, C. Cheng, *Macromolecules,* 2012**, 45**, 4623-4629.
12. B. Zhang, F. Gröhn, J. S. Pedersen, K. Fischer, M. Schmidt, *Macromolecules,* 2006, **39**, 8440-8450.
13. A. E. Levi, J. Lequieu, J. D. Horne, M. W. Bates, J. M. Ren, K. T. Delaney, G. H. Fredrickson, C. M. Bates, *Macromolecules,* 2019, **52**, 1794-1802.
14. X. Zhu, J. Zhang, C. Miao, S. Li, Y. Zhao, *Polym. Chem.,* 2020, **11**, 3003–3017.
15. D. M. Henn, C. M. Lau, C. Y. Li, B. Zhao, *Polym. Chem.*, 2017, **8**, 2702-2712.
16. E. W. Kent, E. M. Lewoczko, B. Zhao, *Langmuir,* 2020, **36**, 13320-13330.
17. B. Gumus, M. Herrera-Alonso, A. Ramírez-Hernández, *Soft Matter*, 2020, **16**, 4969-4979.
18. Y. Yan, X. Fang, N. Yao, H. Gu, G. Yang, Z. Hua, *Macromolecules*, 2022, **55**, 7798-7805.
19. Z. Tang, X. Pan, H. Zhou, L. Li, M. Ding, *Macromolecules,* 2022, **55**, 8668-8675.
20. K. J. Bichler, B. Jakobi, D. Honecker, L. R. Stingaciu, T. K. Weldeghiorghis, J. H. P. Collins, G. J. Schneider, *Macromolecules,* 2022, **55**, 9810-9819.
21. S. Li, P. Liu, Z. Wang, L. Lian, Y. Zhao, *Polym. Chem.*, 2022, **13**, 877-890.
22. G. Chen, E. E. Dormidontova, *Macromolecules,* 2023, **56**, 3286-3295.
23. I. N. Haugan, M. J. Maher, A. B. Chang, T.-P. Lin, R. H. Grubbs, M. A. Hillmyer, F. S. Bates, *ACS Macro Lett.,* 2018, **7**, 525-530.
24. W. F. M. Daniel, G. Xie, M. V. Varnoosfaderani, J. Burdyńska, Q. Li, D. Nykypanchuk, O. Gang, K. Matyjaszewski, S. S. Sheiko, *Macromolecules,* 2017, **50**, 2103-2111.
25. H. Qi, X. Liu, D. M. Henn, S. Mei, M. C. Staub, B. Zhao, C. Y. Li, *Nature Commun.,* 2020, **11**, 2152.
26. A. L. Liberman-Martin, C. K. Chu, R. H. Grubbs, *Macromol. Rapid Commun.*, 2017, **38**, 1700058.
27. W. F. M. Daniel, J. Burdyńska, M. Vatankhah-Varnoosfaderani, K. Matyjaszewski, J. Paturej, M. Rubinstein, A. V. Dobrynin, S. S. Sheiko, *Nature Mater.,* 2016, **15**, 183-189.
28. M. Müllner, *Chem. Commun.,* 2022, 58, 5683-5716.
29. J. A. Johnson, Y. Y. Lu, A. O. Burts, Y. Xia, A. C. Durrell, D. A. Tirrell, R. H. Grubbs, *Macromolecules,* 2010, **43**, 10326-10335.
30. C. A. Salinas-Soto, J. G. Leon-Islas, M. Herrera-Alonso, A. Ramírez-Hernández, *ACS Appl. Polym. Mater.,* 2022, **4**, 7340-7351.
31. A. Detappe, H. V. T. Nguyen, Y. Jiang, M. P. Agius, W. Wang, C. Mathieu, N. K. Su, S. L. Kristufek, D. J. Lundberg, S. Bhagchandani, I. M. Ghobrial, P. P. Ghoroghchian, J. A. Johnson, *Nature Nanotech.,* 2023, **18**, 184-192.
32. X. Banquy, J. Burdyńska, D. W. Lee, K. Matyjaszewski, J. Israelachvili, *J. Am. Chem. Soc.*, 2014, **136**, 6199-6202.
33. V. Adibnia, M. Olszewski, G. De Crescenzo, K. Matyjaszewski, X. Banquy, *J. Am. Chem. Soc.*, 2020, **142**, 14843-14847.
34. G. Xie, P. Krys, R. D. Tilton, K. Matyjaszewski, *Macromolecules,* 2017, **50**, 2942-2950.
35. B. Wang, T. Liu, H. Chen, B. Yin, Z. Zhang, T. P. Russell, S. Shi, *Angew. Chem. Int. Ed.*, 2021**, 60**, 19626-19630.
36. H.-G. Seong, Z. Chen, T. Emrick, T. P. Russell, *Angew. Chem. Int. Ed.,* 2022, **61**, e202200530.
37. M. T. Kelly, Z. Chen., T. P. Russell, B. Zhao, *Angew. Chem. Int. Ed.*, 2023, e202315424.
38. S. S. Sheiko, S. A. Prokhorova, K. L. Beers, K. Matyjaszewski, I. I. Potemkin, A. R. Khokhlov, M. Möller, *Macromolecules,* 2001, **34**, 8354-8360.
39. J. R. Boyce, D. Shirvanyants, S. S. Sheiko, D. A. Ivanov, S. Qin, H. Börner, K. Matyjaszewski, *Langmuir,* 2004, **20**, 6005-6011.

40. F. Sun, S. S. Sheiko, M. Möller, K. Beers, K. Matyjaszewski, *J. Phys. Chem. A*, 2004, **108**, 9682-9686.
41. M. O. Gallyamov, B. Tartsch, A. R. Khokhlov, S. S. Sheiko, H. G. Börner, K. Matyjaszewski, M. Möller, *Macromol. Rapid Commun.*, 2004, **25**, 1703-1707.
42. M. O. Gallyamov, B. Tartsch, A. R. Khokhlov, S. S. Sheiko, H. G. Börner, K. Matyjaszewski, M. Möller, *Chem. Eur. J.*, 2004, **10**, 4599-4605.
43. C. Li, N. Gunari, K. Fischer, A. Janshoff, M. Schmidt, *Angew. Chem. Int. Ed.*, 2004, **43**, 1101-1104.
44. Y. Xu, S. Bolisetty, M. Ballauff, A. H. E. Müller, *J. Am. Chem. Soc.*, 2009, **131**, 1640-1641.
45. H. Luo, M. Szymusiak, E. A. Garcia, L. L. Lock, H. Cui, Y. Liu, M. Herrera-Alonso, *Macromolecules*, 2017, **50**, 2201-2206.
46. S. Y. Joshi, S. Singh, S. A. Deshmukh, *Npj Comput. Mater.*, 2022, **8**, 45.
47. D. M. Henn, W. Fu, S. Mei, C. Y. Li, B. Zhao, *Macromolecules*, 2017, **50**, 1645-1656.
48. E. W. Kent, B. Zhao, *Macromolecules*, 2019, **52**, 6714-6724.
49. E. W. Kent, D. M. Henn, B. Zhao, *Polym. Chem.*, 2018, **9**, 5133-5144.
50. D. M. Henn, J. A. Holmes, E. W. Kent, B. Zhao, *J. Phys. Chem. B*, 2018, **122**, 7015-7025.
51. E. W. Kent, E. M. Lewoczko, B. Zhao, *Polym. Chem.*, 2021, **12**, 265-276.
52. E. M. Lewoczko, M. T. Kelly, E. W. Kent, B. Zhao, *Soft Matter*, 2021, **17**, 6566-6579.
53. M. T. Kelly, E. W. Kent, B. Zhao, *Macromolecules*, 2022, **55**, 1629-1641.
54. K. Zhou, Y. Wang, X. Huang, K. Luby-Phelps, B. D. Sumer, J. Gao, *Angew. Chem. Int. Ed.*, 2011, **50**, 6109-6114.
55. D. M. Henn, R. A. E. Wright, J. W. Woodcock, B. Hu, B. Zhao, *Langmuir*, 2014, **30**, 2541-2550.
56. M. Hu, T. P. Russell, Mater. Chem. Front. 2021, **5**, 1205–1220.
57. M. E. Cates, P.S. Clegg, Soft Matter, 2008, **4**, 2132-2138.
58. T. Majeed, M. S. Kamal, X. Zhou, T. Solling, Energy Fuels 2021, **35**, 5594-5612.
59. E. Glynos, A. Chremos, G. Petekidis, P. J. Camp, and V. Koutsos, Macromolecules, 2007, **40**, 6947-6958.
60. L. Zhao, M. Byun, J. Rzayev, Z. Lin, Macromolecules, 2009, **42**, 9027-9033.
61. A. Chremos, P. J. Camp, E. Glynos, V. Koutsos, Soft Matter, 2010, **6**, 1483-1493.
62. L. Zhao, Z. Lin, Soft Matter, 2011, **7**, 10520-10535.
63. I. L. Geada, H. Ramezani-Dakhel, T. Jamil, M. Sulpizi, H. Heinz, *Nature Commun.*, 2018, **9**, 716.